Handbook of Experimental Pharmacology 246

Mohamed Chahine *Editor*

Voltage-gated Sodium Channels: Structure, Function and Channelopathies

Springer

Handbook of Experimental Pharmacology

Volume 246

More information about this series at http://www.springer.com/series/164

Mohamed Chahine
Editor

Voltage-gated Sodium Channels: Structure, Function and Channelopathies

Springer

Editor
Mohamed Chahine
CERVO Brain Research Center
Institut Universitaire en Santé Mentale
Quebec, Canada

Department of Medicine
Université laval
Quebec, Canada

ISSN 0171-2004 ISSN 1865-0325 (electronic)
Handbook of Experimental Pharmacology
ISBN 978-3-319-90283-8 ISBN 978-3-319-90284-5 (eBook)
https://doi.org/10.1007/978-3-319-90284-5

Library of Congress Control Number: 2018939760

Printed on acid-free paper

This Springer imprint is published by the registered company Springer International Publishing AG part of Springer Nature.
The registered company address is: Gewerbestrasse 11, 6330 Cham, Switzerland

Preface

This is an update and expansion of a previous HEP volume and well-received book entitled *Voltage-Gated Sodium Channels*, edited by Peter Ruben, which details the current state of knowledge of voltage-gated Na^+ channels, their pharmacology, and related diseases. The book chapters authored by internationally recognized experts cover a broad array of topics, including the structural basis of Na^+ channel function, methodological advances in the study of Na^+ channels, the pathophysiology of Na^+ channels, and drug and toxin interactions with these channels.

Na^+ channels play a fundamental role in the initiation and propagation of electrical signals in many excitable cells. Mammalian Na^+ channels are composed of one α-subunit (260 kDa), which forms the core of the channel and is responsible for voltage-dependent gating and ion permeation. The α-subunit is composed of four homologous domains (DI-DIV), each with six α-helical transmembrane-spanning segments (S1–S6). In a state-of-the-art review, Nishino and Okamura present an overview of the molecular and evolutionary aspects of Na^+ channel α-subunits and discuss their contribution to evolutionary changes in animals. The α-subunit forms complexes with auxiliary β-subunits that regulate their trafficking and gating properties. At least four distinct β-subunit subtypes (β1–β4) have been identified. β-subunits are relatively small proteins (33–37 kDa) composed of a single transmembrane α-helix, a short intracellular C-terminus, and a large extracellular N-terminus incorporating an immunoglobulin-like fold similar to that in cell adhesion molecules. The review by Molinarolo et al. summarizes the evolutionary history of β-subunits. Mutations in the genes encoding β-subunits are linked to a variety of diseases, including epilepsy, sudden infant death syndrome, sudden unexpected death in epilepsy, cancer, neuropathic pain, and some major neurodegenerative disorders. Bouza and Isom review the physiopathology of these important regulatory subunits, which also partner with a number of proteins. Balse and Eichel provide an overview of the partners that have been characterized to date, with a focus on the cardiac Na^+ channel. The human genome harbors nine genes encoding voltage-gated Na^+ channels. Mutations in these genes cause dysfunctions of these channels and underlie Na^+ channelopathies. Recent structure–function studies have given us a better understanding of the structural elements of voltage-gated Na^+ channels that are involved in gating and various channel states and drug and toxin

binding sites as well as of the topological arrangement of the channel in the membrane.

Na^+ channel α-subunits are also modulated via posttranslational modifications, including phosphorylation, ubiquitination, palmitoylation, nitrosylation, glycosylation, and SUMOylation. Mercier et al. review the biosynthesis and transport of Na^+ channels as well as the mechanisms involved in their anterograde/retrograde trafficking and subcellular targeting.

Aromolaran et al. review the molecular and structural outcomes of posttranslational modulation (expression, gating, trafficking) of $Na_V1.5$, the cardiac Na^+ channel, through the activation of protein kinase A (PKA) and protein kinase C (PKC), while Pei et al. review all aspects of the posttranslational modification of Na^+ channels. They also discuss the underlying mechanisms of posttranslational modifications that may open the way to the development of new drugs.

Na^+ channels are also regulated by the extracellular pH. Peters et al. review the mechanisms of proton block of the Na^+ channel and the impact this mechanism has on disease states.

Gamal El-Din et al. explore the structural and functional aspects of prokaryotic and eukaryotic Na^+ channels. Payandeh and Hackos reviewed several aspects of structure–function relationships of $Na_V1.7$ Na^+ channel, an important peripheral channel implicated in pain and a promising target for subtype-selective $Na_V1.7$ channel modulators. Na^+ channel dysfunctions cause cardiac arrhythmias, skeletal muscle disorders such as paramyotonia congenita, congenital pain, and neurological disorders.

Na^+ channel mutations are associated with many human channelopathies, including inherited syndromes such as skeletal muscle disorders, which are reviewed by Cannon, and arrhythmic cardiac disorders, which are reviewed by Savio-Galimberti. Mutations in several peripheral Na^+ channels have been shown to underlie congenital pain syndrome (gain-of-function) or lack of pain (loss-of-function); Lampert et al. reviewed the role of these channels in pain. The impact of cell damage on Na^+ channels is modeled and reviewed by Joos et al.

Mutations in the voltage sensor domain of Na^+ channels have been implicated in the generation of leak currents known as gating pore currents or omega currents, which in turn have been implicated in several cardiac and neuromuscular disorders. Groome et al. review the gating pore concept as well as the biophysical properties of gating pores and their involvement in a number of human disorders.

Although the concept of state-dependent drug binding is well accepted, the molecular mechanism underlying this phenomenon is not well understood. The prevailing view is that conformational changes in the local anesthetic drug binding site associated with the voltage-dependent activation and inactivation of Na^+ channels enhance drug binding and stabilize channels in non-conducting states. O'Leary and Chahine review the mechanisms of Na^+ channel gating and the models used to describe drug binding and Na^+ channel inhibition. Farinato et al. present a few other pharmacological aspects of Na^+ channels and summarize the concept of the benzothiazolamine scaffold as an interesting tool to build new Na_v channel

blockers with promising pharmacological and clinical properties. Zhorov et al. summarize the structural models of ligand binding to Na^+ channels.

Natural toxins have long been used as high-affinity probes to study the molecular structure of Na^+ channels. By binding to a precise site, they modify one or more functional properties of Na^+ channels. They can thus be used to probe various components of the channel and study their functional properties. The three-dimensional structures of some toxins are now known, making them powerful tools for probing different regions of the channel or even providing insights into the three-dimensional structures of individual components. Ji summarizes some of the current views on Na^+ channel–toxin interactions.

This book will be of interest to both fundamental and clinical researchers seeking to understand the molecular basis of voltage-gated Na^+ channels as well as those interested in identifying targets for various pharmacotherapies.

Quebec, Canada Mohamed Chahine

Contents

Part I

Evolution of Voltage-Gated Sodium Channels

Evolutionary History of Voltage-Gated Sodium Channels

Atsuo Nishino and Yasushi Okamura

Contents

Abstract

Every cell within living organisms actively maintains an intracellular Na^+ concentration that is 10–12 times lower than the extracellular concentration. The cells then utilize this transmembrane Na^+ concentration gradient as a driving force to produce electrical signals, sometimes in the form of action potentials. The protein family comprising voltage-gated sodium channels (Na_Vs) is essential for such signaling and enables cells to change their status in a regenerative manner and to rapidly communicate with one another. Na_Vs were first predicted in squid and were later identified through molecular biology in the electric eel. Since then, these proteins have been discovered in organisms ranging from bacteria to humans. Recent research has succeeded in decoding the amino acid sequences of a wide variety of Na_V family members, as well as the three-dimensional structures of some. These studies and others have uncovered several of the major steps in the functional and structural transition of Na_V proteins that has occurred along the course of the evolutionary history of organisms. Here we

A. Nishino (✉)
Department of Biology, Faculty of Agriculture and Life Science, Hirosaki University, Hirosaki, Aomori, Japan
e-mail: anishino@hirosaki-u.ac.jp

Y. Okamura
Integrative Physiology, Graduate School of Medicine, Osaka University, Suita, Osaka, Japan

M. Chahine (ed.), *Voltage-gated Sodium Channels: Structure, Function and Channelopathies*, Handbook of Experimental Pharmacology 246,
https://doi.org/10.1007/164_2017_70

present an overview of the molecular evolutionary innovations that established present-day Na_V α subunits and discuss their contribution to the evolutionary changes in animal bodies.

Keywords
Bilaterian · Ca_V · Chordate · Gene duplication · Myelination · Na_V · Vertebrate

1 Introduction

Hodgkin and Huxley in the 1940s–1950s suggested the presence of pores that enabled selective permeation of Na^+ and K^+ ions that was dependent on membrane depolarization and shaped the action potentials (APs). The Na^+-based APs were first recorded from the giant axons of the squid *Loligo* (e.g., Hodgkin and Huxley 1945, 1952). Since then, we have come to recognize voltage-gated Na^+ channels (Na_Vs) as a core element of the nerve impulse that supports essentially all brain function. William A. Catterall and colleagues succeeded in purifying the biochemical component of Na_Vs from rat brains (e.g., Beneski and Catterall 1980; Hartshorne and Catterall 1981; Hartshorne et al. 1985). Noda et al. (1984) isolated a cDNA encoding the pore-forming α subunit of the Na_V from the electric eel, *Electrophorus*. Thereafter, cDNAs for other Na_V α subunits have been cloned from mammals, other vertebrates, and invertebrates. In the fruit fly, *Drosophila melanogaster*, Na_V mutants called *para* were isolated, and the later studies have clearly linked the genotypes of the Na_V α subunit to cellular/whole body-level phenotypes (e.g., Loughney et al. 1989). Then the gene expression of Na_V in response to neural inductive signaling was shown to underlie development of membrane excitability in neurons in a simple chordate model, the ascidian *Halocynthia roretzi* (Okamura et al. 1994). In recent years, Na^+ channels derived from marine bacteria were utilized to increase our understanding of the structural and biophysical basis of Na^+ ion selectivity and voltage dependence (e.g., Payandeh and Minor 2015; Catterall and Zheng 2015). And very recently, genes from the cockroach *Periplaneta* and from *Electrophorus* were utilized to finally resolve the 3D structures of metazoan Na_Vs (Shen et al. 2017; Yan et al. 2017). This brief history of Na^+ channel research reflects the long, but cooperative, struggle to uncover the essence of nature (membrane excitability here) through the use of appropriate biological materials at appropriate times, seemingly making manifest August Krogh's Principle (Krebs 1975).

The aforementioned analyses were performed using Na_Vs from a variety of animal species and demonstrated that the amino acid sequences of the channel proteins have changed to varying degrees and have incorporated innovations in accordance with the evolution of the animals harboring the channels. Given the well-known statement by T. Dobzhansky that nothing in biology makes sense except in the light of evolution, the diversity of Na_Vs provides us with rich insight. Like other gene families, the Na_V gene family grew through gene duplication, sequence changes, and natural selection. These processes now enable animals to utilize similar but independent Na_Vs at different times during development and/or in specific cell types. In this review, we will outline mammalian, vertebrate, chordate, and metazoan Na_V α subunit diversity and the cell type-specific usage

of different isoforms, and we will introduce some of their molecular innovations that correlate with the evolution of animal lifestyles.

2 Structural Outlines of Voltage-Gated Sodium Channels

Metazoan Na_Vs consist of four serially homologous sections, domains I-IV (Fig. 1). Each domain contains six α-helices constituting transmembrane regions S1-S6 linked to each other by extracellular or intracellular loops (Fig. 1a). As a result,

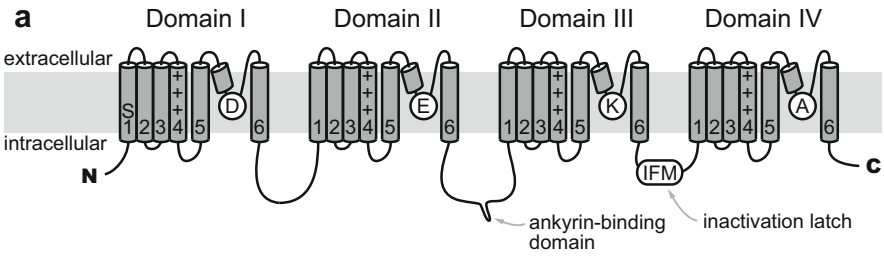

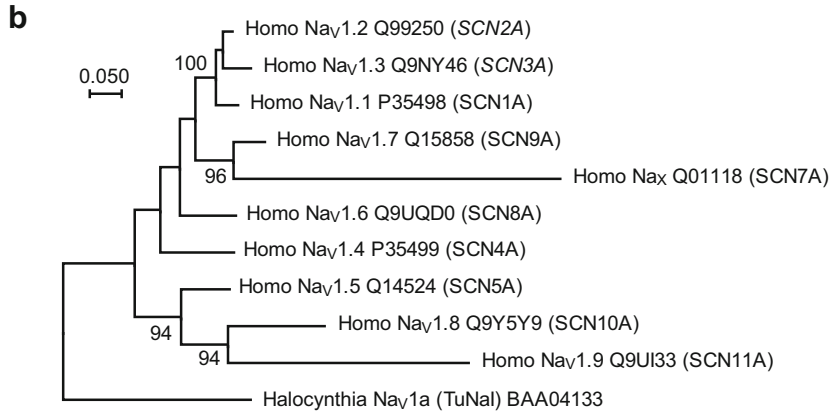

Fig. 1 Mammalian Na_V1 channel α subunits. (**a**) A schematic image of mammalian Na_V1 channels. Diagnostic characteristics of Na_V1s are indicated. Na_V1s have 24 transmembrane segments and are composed of serially homologous domains I–IV, each of which contains segments S1–S6. S4 segments harbor evenly spaced positively charged residues (+). Amino acids at the inner vertices of the loops between S5 and S6 pore-forming segments (P-loops) constitute an ion-selectivity filter. In the case of Na_V1s, the pore signature is Asp/Glu/Lys/Ala (D/E/K/A). The loop between domains II and III contains an ankyrin-binding motif sequence that is reportedly important to localize the Na_V1 channels to the axon initial segment and nodes of Ranvier. The sequence between domains III and IV functions as the inactivation latch (inactivation ball), the core of which is represented by the well-conserved Ile-Phe-Met (I-F-M) triplet. (**b**) A molecular phylogenetic tree of mammalian Na_V1 α subunits constructed by the maximum-likelihood method based on gap-free 1,372 amino acid positions using MEGA7. The sequence from the ascidian *Halocynthia* is used as the out-group. The bootstrap values over 80 are shown. The four groups ($Na_V1.1/1.2/1.3/1.7$, $Na_V1.4$, $Na_V1.6$, $Na_V1.5/1.8/1.9$) are recognized (see text and Table 1)

the full-length metazoan Na_V polypeptide contains a total of 24 transmembrane (TM) regions spanning about 2,000 amino acids. As was proposed for voltage-gated potassium channels (K_Vs), the S1-S4 segments in each domain function as a voltage sensor (e.g., Catterall 2000). In particular, the S4 segment, in which every third amino acid is a positive charged Arg or Lys residue, is considered essential for sensing membrane voltage. In the resting state, S4 is positioned closer to the intracellular side of the membrane. Upon membrane depolarization, S4 moves in an extracellular direction, and this change of conformation stimulates the channel gate to open (Catterall 2000; Shen et al. 2017; Yan et al. 2017). The S5 and S6 segments and the loop between them (P-loop) from each domain occupy a quarter of the central portion of the protein such that the four domains together form the wall, gate, and ion-selectivity filter of the channel (Catterall 2000; Shen et al. 2017).

Mammals, including humans, express nine Na_V isoforms ($Na_V1.1$ to $Na_V1.9$). In addition, a protein most similar to $Na_V1.7$, called Na_X, has also been identified in mammals (Fig. 1b, Table 1). Na_X does not exhibit ion permeability. Instead, it appears to function as a sensor of extracellular Na^+ ion and is now thought to be involved in ionic homeostasis in the body (Hiyama et al. 2002, 2004; Hiyama and Noda 2016). The cDNA sequences, predicted amino acid sequences, locations of the respective encoding genes (*SCN1A-11A*) on the chromosomes, spatiotemporal expression patterns, sensitivity to toxins [e.g., tetrodotoxin (TTX)], single-channel conductances, characteristics of inactivation, and biological functions of these isoforms have all been comprehensively analyzed (some characteristics of mammalian Na_Vs are listed in Table 1) (Goldin 2001; Catterall et al. 2005). For instance, mammalian $Na_V1.1$, 1.2, and 1.3 are encoded by *SCN1A*, *2A*, and *3A*, respectively, and these genes are tandemly arrayed within the genome (on the "q" arm of chromosome 2 in the case of humans) close to the *HoxD* gene cluster (Table 1). The primary structures of these isoforms are mutually similar, suggesting they emerged through relatively recent tandem gene duplications (Fig. 1b). This tandem cluster also includes the gene for $Na_V1.7$ (*SCN9A*), which is expressed in the peripheral nervous system (PNS), including the dorsal root ganglia (DRG)

Table 1 Mammalian voltage-gated sodium channel α subunits[a]

Channel name	Gene symbol	Adj. Hox cluster	Approx. TTX IC_{50}	Tissue to function
$Na_V1.1$	*SCN1A*	*HoxD*	10 nM	CNS
$Na_V1.2$	*SCN2A*	*HoxD*	10 nM	CNS
$Na_V1.3$	*SCN3A*	*HoxD*	10 nM	CNS
$Na_V1.4$	*SCN4A*	*HoxB*	10 nM	Skeletal muscle
$Na_V1.5$	*SCN5A*	*HoxA*	1–10 μM	Heart
$Na_V1.6$	*SCN8A*	*HoxC*	<10 nM	CNS
$Na_V1.7$	*SCN9A*	*HoxD*	10 nM	PNS
$Na_V1.8$	*SCN10A*	*HoxA*	>10 μM	PNS
$Na_V1.9$	*SCN11A*	*HoxA*	1 μM	PNS
Na_X	*SCN7A*	*HoxD*	–	CNS and others

[a]This table is modified from Goldin (2001)

(Sangameswaran et al. 1997; Toledo-Aral et al. 1997). The gene encoding Na_X (*SCN7A*) is also found in this cluster. $Na_V1.7$ and Na_X constitute a sister clade in the molecular phylogenetic tree, and the duplication of these two genes occurred in parallel with the splits of $Na_V1.1$, 1.2, and 1.3 (Fig. 1b) (Catterall et al. 2005). They commonly show high sensitivity to TTX, with IC_{50}s around 10 nM (summarized in Goldin 2001). In addition to the channels already mentioned, the central nervous system (CNS) expresses $Na_V1.6$, which exhibits characteristic persistent current and a large resurgent current, while the PNS expresses $Na_V1.8$ and 1.9. The heart expresses $Na_V1.5$, encoded by *SCN5A*, which clusters with *SCN10A* encoding $Na_V1.8$ and *SCN11A* encoding $Na_V1.9$, close to the *HoxA* cluster (Table 1). $Na_V1.8$ and 1.9 are also presumed to have emerged through tandem gene duplication that occurred after the two rounds of whole genome duplication in the ancestor of jawed vertebrates (see below) and share relatively slow activation kinetics (Fig. 1b) (Lai et al. 2004). Along with $Na_V1.5$, $Na_V1.8$ and 1.9 are relatively insensitive to TTX, with IC_{50} in the range of 1–10 μM or more (Gellens et al. 1992; Akopian et al. 1996; Tate et al. 1998). Skeletal muscles use $Na_V1.4$ for APs, and its gene, *SCN4A*, is not clustered with other Na_V genes and neighbors the *HoxB* cluster (Table 1). $Na_V1.4$ in skeletal muscle is as sensitive to TTX as Na_Vs in the CNS (NaV1.1–1.3, and 1.6).

All nine Na_Vs possess an activation gate that opens in response to membrane depolarization and an ion-selectivity filter that enables selective Na^+ permeation. The extracellular fluid around living cells generally contains a high concentration of Na^+, while the intracellular fluid has a lower Na^+ concentration. Na_V gating allows Na^+ to flow into the cell and depolarize the membrane, though the channel soon shuts through the process of inactivation. The inactivation function is one that the Na_V α subunits themselves possess and enables immediate repolarization of the membrane to sharpen the AP (Hodgkin and Huxley 1952). All known Na_Vs show some degree of inactivation, which is known to require the linker sequence between domains III and IV (Stühmer et al. 1989), a region called the "inactivation ball" or "inactivation latch" (Fig. 1a). The latch is modeled to fit into the open pore and block ion permeation (ball-and-chain model). Within the sequence of this linker, three consecutive hydrophobic amino acids, Ile-Phe-Met, are well shared by vertebrate Na_Vs and are totally conserved in all the human Na_V isoforms. This triplet, especially the central Phe residue, is essential for inactivation, and thus hydrophobic interaction between the latch and the open pore would be important (West et al. 1992; see also a recent revision to this model proposed from the structural study by Yan et al. 2017).

The P-loop between S5 and S6 in each of the four domains protrudes into the central canal of Na_Vs, and the inner vertices of the loops are thought to constitute the ion-selectivity filter (Heinemann et al. 1992; Shen et al. 2017). The residues for Na^+ ion selectivity in all mammalian Na_Vs are Asp from domain I, Glu from domain II, Lys from domain III, and Ala from domain IV (asymmetric D/E/K/A signature) (Fig. 1a). By contrast, most Ca_Vs, which have a similar 24-TM conformation, show a symmetric E/E/E/E pore signature (e.g., Hinemann et al. 1992). The 3–4 acidic residues behind the D/E/K/A signature residues (E/E/D/D in all

mammalian Na_Vs) form the "outer ring," which is also significant for positively charged ion permeability (Catterall 2000). The region around the signature residue in domain I is a definitive binding target for TTX (Noda et al. 1989). This selectivity filter is located midway through the canal, and the outer ring is a bit extracellular to the signature. On the intracellular side is a central cavity enclosed by charged residues, with the predicted activation gate composed of the S6 segments from domains I-IV aligned along the channel fenestration (Catterall 2000; Shen et al. 2017).

These structural features, including the 24-TM segments in the four serially homologous domains, the voltage-sensor domains, D/E/K/A selectivity filter, central cavity, activation gate, and inactivation latch are shared by all mammalian Na_V α subunits (e.g., Catterall 2000; Catterall et al. 2005).

3 Historical Origin of Voltage-Gated Sodium Channels and Their Related Proteins

The discovery of Na_Vs in bacteria (BacNa_Vs) confirmed that Na^+-permeable channel proteins gated in response to changes in membrane potential had already evolved in prokaryotes (Ren et al. 2001; Payandeh and Minor 2015). However, these BacNa_Vs are composed of homotetrameric 6-TM subunits that contain compact S1-S6 segments (e.g., Payandeh and Minor 2015; Catterall and Zheng 2015). Because a BacNa_V can be changed into Ca^{2+}-selective channel through simple mutation(s), it is thought that prokaryotes can also possess voltage-gated Ca^{2+} channels (Yue et al. 2002). In addition, the K_VAP channel, the first voltage-gated ion channel whose structure was resolved, is a K^+ channel from prokaryotic archaea (Jiang et al. 2003). It is thus evident that prokaryotes likely made use of a wide variety of voltage-gated, ion-specific 6-TM channels long before the emergence of eukaryotes. The 6-TM segments can be functionally divided into a voltage-sensing unit composed of segments S1-S4 and an ion channel pore domain corresponding to segments S5-S6, including the P-loop in between. Members of the prokaryotic KcsA-related channel and eukaryotic Kir channel families are composed of homotetrameric 2-TM helices, which are thought to represent units of the tetraradial pore domains (e.g., Bichet et al. 2003). The K2P channel family members show a tandem repeat of two pore domains, dimerization of which produces a channel pore of pseudotetrameric symmetry (e.g., Honoré 2007). Recent research has revealed that the voltage-sensor domain can also function independently of the pore domain. For instance, the recently identified voltage-sensing phosphatase (VSP) possesses S1-S4-like segments coupled to phosphatase domain that catalyze membrane phospholipid dephosphorylation in response to changes in membrane potential (Murata et al. 2005). It is also known that the primary structure of a voltage-dependent proton channel, H_V1/voltage-sensor-domain-only protein (VSOP), is comparable to segments S1-S4 of 6-TM voltage-gated ion channel subunits (Ramsey et al. 2006; Sasaki et al. 2006).

All of the prokaryotic voltage-gated ion channels identified so far are composed of homotetrameric 6-TM subunits. Eukaryotic voltage-gated K^+ channels

and Ca^{2+}-permeable Catsper channels are still tetrameric compositions of 6-TM subunits (Liebeskind et al. 2013). In addition to these, eukaryotes express larger voltage-gated ion channel proteins composed of 12-TM or 24-TM segments. The 12-TM channels are two-pore channels (TPCs), which are cation channels functioning within intracellular organelles such as endosomes and lysosomes (Calcraft et al. 2009). The 24-TM ion channel family includes not only Na_Vs but also L-, T-, and N/P/Q/R-type Ca_Vs (also called Ca_V1, Ca_V2, and Ca_V3, respectively) and cation leak channels (NALCN). It is thought that eukaryotic 24-TM channels harboring four-time serially homologous domains are derived from two rounds of tandem duplication of an original 6-TM factor. In fact, the amino acid sequences of domain I of the Na_V and Ca_V1, 2, and 3 channels are more similar to domain III than to II or IV, while the sequence in domain II is more like that of IV than domain I or III (Strong et al. 1993; Liebeskind et al. 2013). It is also known that the amino acid sequences of these four domains are closer to each other, and to those of the Catsper isoforms, than to the sequences of $BacNa_V$s or K_Vs. These relationships suggest eukaryotic 24-TM channels were not derived from duplication of a $BacNa_V$, but arose instead through two sequential rounds of duplication of a gene encoding a Catsper-like 6-TM protein; one duplication gave rise to a gene encoding 12-TM segments containing domain I and II, and a second tandem duplication established the present conformation composed of domains I-IV (Liebeskind et al. 2013). This process was significant in that the ion channel molecules got to be formed by a single polypeptide stretch, not by four identical subunits, which would facilitate accumulation of "asymmetric" mutations independently within domains I to IV to make the channel "pseudotetrameric." This implies that this process would potentiate future molecular evolutionary fine-tuning for specific functions – e.g., Na^+ selectivity, fast inactivation, anchoring, etc. (see below).

In addition to the channels mentioned to far, another 24-TM subfamily, Na_V2, has been identified in invertebrates, and its members have amino acid sequences similar to Na_V1, but exhibits a D/E/E/A pore signature (Salkoff et al. 1987; Sato and Matsumoto 1992; Nagahora et al. 2000; Zhou et al. 2004; Zakon 2012; Gur Barzilai et al. 2012; Moran et al. 2015). Later analyses proved that the members of this family are permeable to Ca^{2+}, and it has recently been proposed that this family be renamed Ca_V4 (Zhou et al. 2004; Gosselin-Badaroudine et al. 2016). It has also been reported that a mutant $Na_V1.2$ channel of rat giving a D/E/E/A pore signature is permeable not only to Na^+ but also to Ca^{2+} and K^+ and that the presence of a physiological concentration of Ca^{2+} in the extracellular fluid blocks permeation of Na^+ through the mutant channel (Heinemann et al. 1992). This nonselective permeation of cations is also observed in a cnidarian Na_V family channel having the D/E/E/A pore (called $NvNa_V2.1$), although it does not show the blockade by extracellular Ca^{2+} (Gur Barzilai et al. 2012). Given its sequence similarity to Na_V1 and its functional characteristics, we will refer to this subfamily as $Na_V2(Ca_V4)$ here.

The major diversification events of these families of 24-TM channels of animals, namely, evolutionary splits of the Na_V, Ca_V, and NALCN families, predate the origin of metazoan animals (Fig. 2a). The split of the $Na_V1/Na_V2(Ca_V4)$ clade from the Ca_V1–3 molecular clades occurred before the divergence of animals and

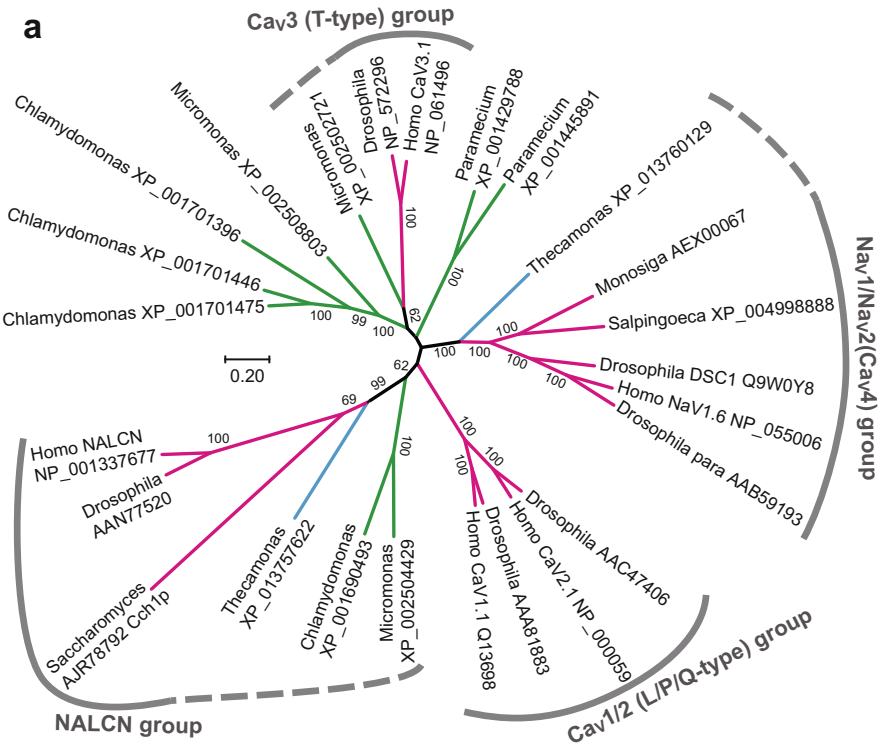

b

				Domain I	Domain II	Domain III	Domain IV
NALCN group	Chlre	XP_001690493		TLTGW	NLENW	TLNGY	TGDNW
	Thetr	XP_013757662		TLEGW	AGDAW	SLEGW	TGEDW
	Sacce	AJR78792		SANTF	STENW	SLEGW	FGEGW
	Drome	AAN77520		SQEGW	TQEAW	SFKGW	TGEDW
	Homsa	NP_001337677	NALCN	SQEGW	TQEGW	SLKGW	TGEDW
$Ca_V1/2$ group	Drome	AAC47406		TMEGW	TGEDW	TGEGW	TGEAW
	Homsa	NP_000059	CaV2.1	TMEGW	TGEDW	TGEGW	TGEAW
	Drome	AAA81883		TLEGW	TGEDW	TFEGW	TGEAW
	Homsa	Q13698	CaV1.1	TMEGW	TGEDW	TFEGW	TGEAW
$Na_V1/2$ group	Thetr	XP_013760129		TMDEW	IGE-W	TFEGW	TASGW
	Monbr	AEX00067		TLDFW	CGE-W	TFEGW	TGAGW
	Salro	XP_004998888		LLDFW	CCE-W	TFEGW	TAAGW
	Drome	Q9W0Y8	DSC1	TLDYW	CGE-W	TFEGW	TSAGW
	Homsa	NP_055006	NaV1.6	TQDYW	CGE-W	TFKGW	TSAGW
	Drome	AAB59193	para	TQDFW	CGE-W	TFKGW	TSAGW
Ca_V3 etc.	Parte	XP_001429788		TTEGW	TNESW	TTEGW	TGEDW
	Micco	XP_002502721		TLEGW	TGEDW	TTEGW	TGEAW
	Drome	NP_572296		SLEGW	TQEDW	SRDGW	TGDNW
	Homsa	NP_061496	CaV3.1	TLEGW	TQEDW	SKDGW	TGDNW
	Micco	XP_002508803		SMEGW	TGENW	TLEGW	TGEAW
	Chlre	XP_001701475		TQEGW	TMENW	TLELW	TGESW
	Chlre	XP_001701446		TLSGW	TGENW	TMSLW	TGESW

Fig. 2 Molecular phylogeny of eukaryotic 24-TM channels. (**a**) An unrooted maximum-likelihood tree of 24-TM channels found in green algae (*Chlamydomonas reinhardtii*, *Micromonas commoda*), the ciliate (*Paramecium tetraurelia*), the fungi (*Saccharomyces cerevisiae*), the apusozoan flagellate (*Thecamonas trahens*), choanoflagellates (*Monosiga brevicollis*, *Salpingoeca rosetta*), and metazoans (*Drosophila melanogaster*, *Homo sapiens*). Accession numbers of the

choanoflagellates, the protozoan group most closely related to the metazoan clade (Zakon 2012; Liebeskind et al. 2012; Moran et al. 2015). NALCN-like sequences are also found in fungi, and the history of this family can be traced back to the origin of opisthokonta, the monophyletic group containing animals, choanoflagellates, and fungi (Torruella et al. 2011; Liebeskind et al. 2012). Figure 2a shows here that in fact the representative unicellular eukaryotes distantly related with each other, such as the yeast *Saccharomyces*, the ciliate *Paramecium*, and green algae *Chlamydomonas* and *Micromonas*, possess different types of the 24-TM channel proteins. For instance, *Saccharomyces*, *Chlamydomonas*, and *Micromonas* express a 24-TM channel related to NALCN of animals, while *Paramecium*, *Chlamydomonas*, and *Micromonas* use other types of 24-TM channels closer to Na_Vs or Ca_Vs of animals (Fig. 2a). This suggests that the gene duplication of NALCN, Na_V, and Ca_V (even between $Ca_V1/2$ and Ca_V3) families preceded the split of Unikonta (including animals, fungi, and amoebozoans) and Bikonta (plants, algae, etc.), namely, had occurred close to or before the origin of eukaryotes (Fig. 2a) (see also the phylogenetic views of eukaryotic lineages in Roger and Simpson 2008; Rogozin et al. 2009; Cavalier-Smith 2010). Despite the deep origin of the voltage-gated 24-TM Ca^{2+}/Na^+ channels, it is also known that many eukaryotic groups lack the genes of them, probably because of secondary loss. Brunet and Arendt (2015) argued that the losses of 24-TM Na_V/Ca_V channels that had happened in varied eukaryote lineages are tightly correlated with the absence of flagella in those organisms. The Ca_V channels of *Paramecium* and *Chlamydomonas* are localized in the membrane of their cilia/flagella, in which the channels function to generate APs to change flagellar/ciliary beating waveforms (Machemer and Ogura 1979; Fujiu et al. 2009). The flagellar localization of the 24-TM Ca_V/Na_V channels may be a preadaptation for the later emergence of neurons (Brunet and Arendt 2015).

While the phylogenetic relationships among the protein sequences from various eukaryotes are based on overall sequence similarities, the ion-selectivity filter signatures (D/E/K/A, E/E/E/E, E/E/D/D, and E/E/K/E in mammalian Na_V1, $Ca_V1/2$, Ca_V3, and NALCN, respectively) were established relatively recently (Fig. 2b) (Liebeskind et al. 2011, 2012). This means that the specific ion selectivity of each family may have changed over the course of evolution. For instance, the D/E/K/A pore signature of Na_V1 is thought to have emerged at the origin of

Fig. 2 (continued) sequences are indicated in the tree. The groups of $Na_V1/Na_V2(Ca_V4)$, $Ca_V1/2$, Ca_V3, and NALCN and their extended clades are indicated with *gray* solid and *dashed lines*. The bootstrap values over 60 are shown. The tree was constructed using the WAG model on MEGA7 from gap-free 847 amino acid positions aligned by MUSCLE program. (**b**) The pore signatures (at the putative ion-selectivity filter in the P-loops) of the eukaryotic 24-TM channels. The signature sequences were obtained from the alignment used for constructing the tree shown in (**a**). The species codes (first column) made of the first three and two letters from the genus and species name, respectively, and accession numbers (second column) are shown. The amino acids at the pore signatures are highlighted with colors [Asp (D), *magenta*; Glu (E), *red*; Lys (K), *blue*; Ala (A), *yellow*; other polar amino acids, *green*]

Bilateria (the clade of animals with bilateral body plans). The evidence is that all Na_V-type 24-TM genes found so far in choanoflagellates (the closest relatives to metazoans) (*Monosiga* and *Salpingoeca* in Fig. 2) and in ctenophores and placozoans (non-bilaterian metazoans), encode the D/E/E/A filter motif, not D/E/K/A, which implies the $Na_V2(Ca_V4)$-type pore signature is original (Liebeskind et al. 2011; Zakon 2012; Gur Barzilai et al. 2012; Moran et al. 2015). Cnidarians, another major non-bilaterian metazoan group, express several isoforms of Na_V-like 24-TM polypeptides with D/E/E/A (called $Na_V2.1$, 2.3, and 2.4), D/E/E/T ($Na_V2.2$), and D/K/E/A ($Na_V2.5$) pore signatures, and a phylogenetic analysis suggested that the latter two of the isoforms were derived from the first (Fig. 3) (Gur Barzilai et al. 2012; Moran et al. 2015). The cnidarian D/K/E/A channels ($Na_V2.5$) are presumably Na^+-selective, representing convergent evolution of Na^+-selective channels that was independent from the origin of the D/E/K/A Na_V1 subfamily in bilaterians (see below) (Anderson et al. 1993; Gur Barzilai et al. 2012). This molecular parallel evolution may be related to independent acquisitions of large bodies moving fast in cnidarians (e.g., jellyfish) and in bilaterians. On the other hand, the pore signature of cnidarian NALCN-like genes is commonly E/E/E/E, which likely ensures Ca^{2+} selectivity, while those in all known bilaterians have E/E/K/E at the selectivity filter, making the channels to be cation nonselective (Lu et al. 2007; Liebeskind et al. 2012).

From the evidence summarized above, it can be predicted that at their origin animals possessed two or three Ca_V subfamily genes, one $Na_V2(Ca_V4)/Na_V1$ subfamily gene and one NALCN-like gene (Moran and Zakon 2014; Moran et al. 2015). Interestingly, none of the channels are Na^+-selective, but are Ca^{2+}-preferential. Animals may have evolved as organisms lacking voltage-gated Na^+-selective channels, and the true metazoan Na^+ channels, Na_V1s with the D/E/K/A signature, emerged in a bilaterian ancestor via gene duplication and diversification that at the same time gave rise to the $Na_V2(Ca_V4)$ subfamily.

4 Evolution of Bilaterians and Voltage-Gated Sodium Channel Proteins

Bilateria is composed of animals having bilateral body plans, which are classified into three superphyla, Deuterostomia, Lophotrochozoa, and Ecdysozoa. These animal groups share a basic repertoire of 24-TM ion channel paralogues of three subtypes of Ca_V (Ca_V1–3), two of $Na_V1/Na_V2(Ca_V4)$, and one of NALCN leak channel. The molecular phylogenetic analysis suggests that the Na_V1 subfamily was diverged from the $Na_V2(Ca_V4)$ subfamily and originated in the last common ancestor of bilaterians (Fig. 3) (Liebeskind et al. 2011; Moran et al. 2015). The origin of Na_V1 in fact correlated with the development of the D/E/K/A pore signature and therefore represents the occurrence of "true" Na^+ selectivity in 24-TM channels (Fig. 3) (Liebeskind et al. 2011). This channel enabled bilateral animals to specifically utilize Na^+, the most abundant cation within the environment in which they had adapted. Combined with the function of the Na^+ pump (Na,K-ATPase), Na_V1 would have conferred a fast electric responsiveness to excitable cells by means of the large

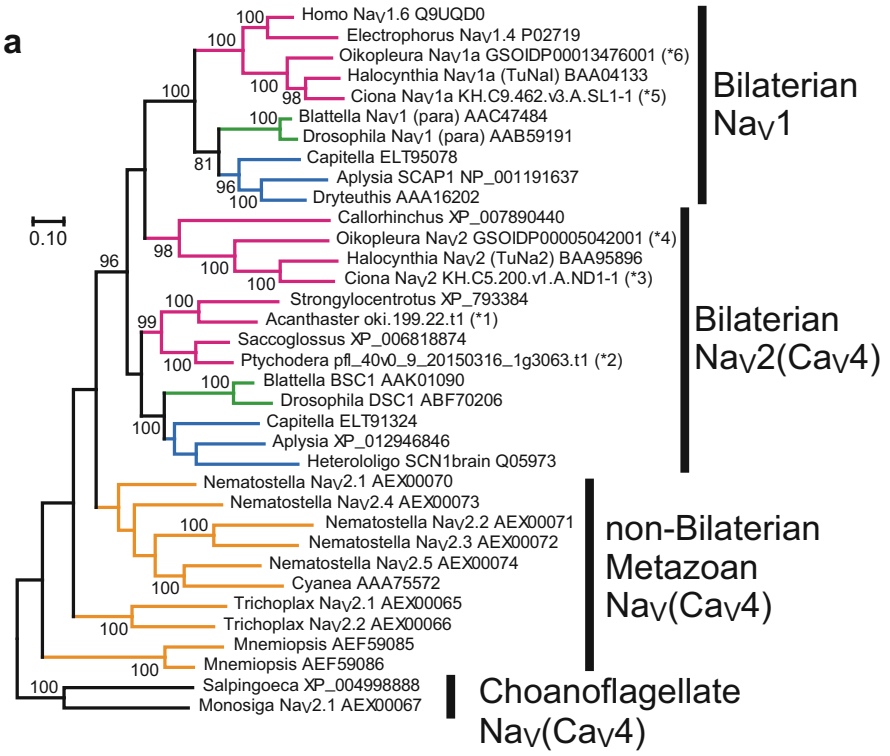

b

				Domain I	II	III	Inactivation latch	IV
Ctenophora	Mnele	AEF50086		TLDFW	CGEWI	XXXXX	GQLGVLLTPAQ	TSAGW
Ctenophora	Mnele	AEF59085		XXXXX	CGEWI	TFEGW	GQLGVLLTPGQ	TSAGW
Placozoa	Triad	AEX00065	NaV2.1	TLDNW	CGEWI	TFEGW	IPTDLFMTESQ	TSAGW
Placozoa	Triad	AEX00066	NaV2.2	TMDFW	CGESV	TFEGW	IPTDILLTESQ	TAAGW
Jellyfish	Cyaca	AAA75572		TLDYW	CGKWI	TLEGW	DGVGIFLTPGQ	TAAGW
SeaAnemone	Nemve	AEX00070	NaV2.1	TMDFW	CGEWI	TFEGW	GALDIFLTPSQ	TSAGW
SeaAnemone	Nemve	AEX00071	NaV2.2	TMDFW	CSEWV	TYEGW	NSMGMLLTESQ	TGTGW
SeaAnemone	Nemve	AEX00072	NaV2.3	TLDFW	CGEWI	TFEGW	SGMGMLLTERQ	TGAGW
SeaAnemone	Nemve	AEX00073	NaV2.4	TLDFW	CGEWI	TFEGW	GSMDVFLTSTQ	TSAGW
SeaAnemone	Nemve	AEX00074	NaV2.5	TMDYW	CGKWI	TLEGV	GSLGFLLTASQ	TAAGW
Cockroach	Blage	AAK01090	BSC1	TLDYW	CGEWT	TFEGW	GVLEMFLTESQ	TSAGW
FruitFly	Drome	ABF70206	DSC1	TLDYW	CGEWI	TFEGW	GVLEVFLTESQ	TSAGW
Annelid	Capte	ELT91324		TLDFW	CGEWI	TFEGW	GYVDVLLTPSQ	TAAGW
Squid	Hetbl	Q05973		TQDYW	CGEWI	TFEGW	TYLDMFLTPTQ	TSAGW
SeaSlug	Aplca	XP_012946846		TLDFW	CGEWI	TFEGW	SYLDAFLTQSQ	TAAGW
SeaUrchin	Strpu	XP_793384		TLDYW	CGEWI	TFEGW	SSMDMLLSTSQ	TSAGW
Starfish	Acapl	*1		TLDFW	CGEWI	TFEGW	SSFGLFLTSNQ	TSAGW
AcornWorm	Sacko	XP_006818874		TLDYW	CGEWI	TFEGW	NTLDMFLTSSQ	TSAGW
AcornWorm	Ptyfl	*2		TLDFW	CGEWI	TFEGW	STLDMFLTSNQ	TSAGW
Ascidian	Cioin	*3	NaV2	TLDYW	CGEWI	TFEGW	SAVEALLTDNQ	TSAGW
Ascidian	Halro	BAA95896	NaV2/TuNa2	TLDYW	CGEWI	TFEGW	SAVEAFLTESQ	TSAGW
Larvacean	Oikdi	*4	NaV2	TLDFW	CGEWV	TFEGW	SACDTIMTPEQ	TSAGW
Shark	Calmi	XP_007890440	NaV2	TLDYW	CGEWI	TFEGW	GALVTLLTEDQ	TAAAW
Cockroach	Blage	AAC47484	para	TQDYW	CGEWI	TFKGW	GSLEMFMTEDQ	TSAGW
FruitFly	Drome	AAB59191	para	TQDFW	CGEWI	TFKGW	GSLEMFMTEDQ	TSAGW
Annelid	Capte	ELT95078		TQDYW	CGEWI	TFKGW	GSLEMFMSEDQ	TSAGW
Squid	Dorop	AAA16202		TQDYW	CGEWI	TFKGW	GSLEVFMTDDQ	TSAGW
SeaSlug	Aplca	NP_001191637	SCAP1	TQDFW	CGEWI	TYKGW	GSLEMFMTEDQ	TSAGW
Ascidian	Cioin	*5	NaV1a	AQDYW	CGEWI	TFKGW	GGQDIFMTEEQ	TSAGW
Ascidian	Halro	BAA04133	NaV1a/TuNaI	AQDYW	CGEWI	TYKGW	GGQDIFMTEEQ	TSAGW
Larvacean	Oikdi	*6	NaV1a	VQDYW	CGEWI	TFKGW	GGQDIFMTEEQ	TSAGW
Teleost	Eleel	P02719	NaV1.4	LQDYW	CGEWI	TFKGW	GGEDLFMTEEQ	TSAGW
Mammal	Homsa	Q9UQD0	NaV1.6	TQDYW	CGEWI	TFKGW	GGQDIFMTEEQ	TSAGW

Fig. 3 Molecular phylogeny of metazoan $Na_V1/Na_V2(Ca_V4)$ channels. (**a**) A maximum-likelihood tree of Na_V-related channels from the ctenophore (*Mnemiopsis leidyi*), the placozoan (*Trichoplax adhaerens*), the jellyfish (*Cyanea capillata*), the sea anemone (*Nematostella vectensis*), squids

driving force across the membrane. Na_V1 would also be important in that it could mediate steep depolarization without direct stimulation of the intracellular processes triggered by Ca^{2+}, a major second messenger in the wide variety of unicellular and multicellular organisms. It is also possible the inactivation latch in the loop between domains III and IV developed at the same time (Fig. 3b), which would have facilitated fast recovery to the resting state of membrane potential and thus enabled cells to minimize the changes in intracellular ionic conditions. Importantly, the molecular development of Na_V1 would be related not only to fast generation/propagation of APs but also to the occurrence of refractory periods after depolarization. Repetitive excitation of neurons is facilitated by these characteristics of Na_V1, which enables the nerves to encode neural signals based on the AP frequencies. Fast neural transmission would have supported evolution of larger bodies, and the ability to inactivate itself can ensure unidirectional flow of signals within the neural network. This would have offered segregation of input (sensory) systems from output (motor) systems, permitting development of the CNS.

The evolutionary emergence and divergence of bilaterians represents the geographical event called the "Cambrian explosion." It is inspiring to consider that the origin of Na_V1 is concordant with the evolution of bilaterians. Paleontologists have suggested that predator-prey relationships were established during the Cambrian era, which stimulated increases in body size and complexity and also the sophistication of sensory organs, leading to acceleration of movement and further elaboration of the CNS (Conway-Morris 1986; Gould 1990; Parker 2003). One hypothesis has proposed that development of eyes was a key step in this so-called evolutionary big bang (Parker 2003). Given this context, it would be reasonable to predict that

Fig. 3 (continued) (*Doryteuthis opalescens*, *Heterololigo bleekeri*), the sea slug (*Aplysia californica*), the annelid worm (*Capitella teleta*), the fruit fly (*Drosophila melanogaster*), the cockroach (*Blattella germanica*), acorn worms (*Ptychodera flava*, *Saccoglossus kowalevskii*), the starfish (*Acanthaster planci*), the sea urchin (*Strongylocentrotus purpuratus*), ascidians (*Ciona intestinalis*, *Halocynthia roretzi*), the larvacean (*Oikopleura dioica*), the elephant fish chimaera (*Callorhinchus milii*), the electric eel (*Electrophorus electricus*), and humans (*Homo sapiens*). Monophyly of bilaterian Na_V1s is evident, while that of $Na_V2(Ca_V4)$ channels is not clear here. The sequences from non-bilaterian metazoans, ecdysozoans, lophotrochozoans, and deuterostomes are labeled with *yellow*, *blue*, *green*, and *magenta* branches, respectively. NCBI accession numbers and other ID codes are indicated in the tree. The sequences of *O. dioica* are obtained from OikoBase (http://oikoarrays.biology.uiowa.edu/Oiko/); those of *C. intestinalis* are from Ghost database (http://ghost.zool.kyoto-u.ac.jp/cgi-bin/gb2/gbrowse/kh/); those of *A. planci* and *P. flava* are from the OIST genome browsers (http://marinegenomics.oist.jp/gallery/gallery/index). The bootstrap values over 80 are shown. The tree was constructed using the WAG model on MEGA7 from gap-free 812 amino acid positions aligned by MUSCLE program. (**b**) The pore signatures and the region corresponding to the inactivation latch in metazoan Na_V-related channels. The sequences shown are mostly identical to those in (**a**). The species codes and color codes are same as in Fig. 2. Sequences corresponding to core triplet of the inactivation latch (I-F-M) are also marked by *purple*. *Cyan* residues indicate the amino acids identical to those around the inactivation latch of the mammalian $Na_V1.6$. *1-*6: the genemodel IDs are shown in (**a**) to identify the sequences in the genome browser of each organism

the molecular phylogenetic origin of Na_V1 provided a physiological basis for the bilaterian ancestor that potentiated the explosive evolution.

Na_V1 originated through gene duplication and diversification that gave rise to the $Na_V2(Ca_V4)$ as well (Fig. 3a). Consequently, most bilaterians express two subtypes of Na_V family components, Na_V1 and $Na_V2(Ca_V4)$. For example, the genome of *Drosophila melanogaster* harbors *para*, which encodes a Na_V1-type channel, and *DSC1*, which encodes a $Na_V2(Ca_V4)$ channel (Salkoff et al. 1987; Ramaswami and Tanouye 1989; Loughney et al. 1989; Hong and Ganetzky 1994; Kulkarni et al. 2002; Zhang et al. 2013). Major invertebrate lineages, such as mollusks, annelids, arthropods, and chordates all express $Na_V2(Ca_V4)$ proteins in addition to Na_V1. $Na_V2(Ca_V4)$ family proteins contain voltage sensors – i.e., S4 segments containing evenly spaced, positively charged residues, and their pore signature is generally D/E/E/A. When exogenously expressed in *Xenopus* oocytes, $Na_V2(Ca_V4)$ family proteins from the cockroach and honeybee (called BSC1 and $AmCa_V4$, respectively) are more permeable to the divalent cations Ca^{2+} and Ba^{2+} than to Na^+ (Zhou et al. 2004; Gosselin-Badaroudine et al. 2016). These channels are reportedly insensitive to TTX, exhibit relatively slow activation and inactivation, and can be blocked by Cd^{2+} or Zn^{2+}. Phenotypic analyses of *DSC1* gene mutants in *Drosophila* have suggested its functions in olfaction or odor-responsive behavior and also in stabilizing the performance of neural circuits under stresses (Kulkarni et al. 2002; Zhang et al. 2013).

While bilateral animals share orthologues of Na_V1 and $Na_V2(Ca_V4)$, it has also been revealed that some animal lineages have lost either the Na_V1 or $Na_V2(Ca_V4)$ subtype, or both. It is well known, for example, that the genome of *Caenorhabditis elegans* contains neither Na_V1 nor $Na_V2(Ca_V4)$ (e.g., Okamura et al. 2005). Whether these paralogues are present or absent is thought to reflect the physical characteristics and lifestyle of each animal group, including body size, locomotion speed, and/or complexity of neural processing. Although the nematode lacks any Na_V-class channels, it is not true that this species is "primitive." The nematode lost this protein because it was not essential for its interstitial life. In fact, nematodes have flourished around the globe without it.

The Na_V1 family channels are absent from echinoderms and hemichordates, the group collectively called Ambulacraria, which constitutes the sister clade of the phylum Chordata (Fig. 3) (see also Widmark et al. 2011; Gur Barzilai et al. 2012). This indicates that echinoderms and hemichordates (ambulacrarians) secondarily lost the fast Na_V1, while the $Na_V2(Ca_V4)$ with the D/E/E/A pore signature typical for that subfamily remains. This suggests these animal groups are incapable of fast sodium spikes. These animals are small during the larval stage (about 0.1–5.0 mm), and the adults (about 1–10 cm or more sometimes) are generally slow moving. They are not fast predators but protective; echinoderm adults are covered with calcite skeletons, and sometimes also with spines, while hemichordates are generally buried in the seafloor. They develop an ectodermal nerve net over the entire body, and their CNS is relatively rudimentary (Hyman 1955; Holland 2003, 2016; Nomaksteinsky et al. 2009). Their evolutionary status may be regarded like an atavism – i.e., reminiscent of the status of animals before the origin of bilaterians. In other words,

they live a "slow life" that is a consequence of the loss of Na_V1. On the contrary, the last common ancestor of bilaterians had a Na_V1-type channel and lived a "quick life." Therefore, the long-standing controversy around how the less centralized nervous system seen in echinoderms or hemichordates was integrated into the well-centralized nervous system of vertebrates may not be valid (for reviews, e.g., Holland 2003, 2016). It is noteworthy that recent analyses of the CNS of a polychaete annelid (ragworm) provided surprising evidence of its deep anatomical similarity to the vertebrate CNS (Tessmar-Raible et al. 2007; Tomer et al. 2010; Vergara et al. 2017). A well-centralized nervous system in the last common ancestor of bilaterians would be consistent with the evolution of Na_V1.

5 Voltage-Gated Sodium Channels in Chordates

As the bilaterians diversified, the chordate lineage led to vertebrates and two other animal groups, the amphioxi (cephalochordates, lancelets) and tunicates (urochordates). Recent comparative genomic analyses showed that the amphioxi diverged first within these three groups, and tunicates and vertebrates form a sister group (Delsuc et al. 2006; Putnam et al. 2008). Amphioxi and tunicates provided "observation windows" for researchers to investigate past situations before establishment of vertebrate bodies.

Amphioxi inhabit sandy shores and live as filter feeders. They are able to swim out of the sand and dive back into it very quickly. While they develop segmented somites, they lack developed eyes or an expanded brain (Willey 1894). Their repertoire of Na_V-related α subunits also appears primitive. An amphioxus likely possesses five genes encoding $Na_V1/Na_V2(Ca_V4)$ channel α subunits. At least three of the genes are classified as Na_V1 family, and the other two are in the $Na_V2(Ca_V4)$ clade (Fig. 4a). The three Na_V1 channels of amphioxi are paralogous with each other and share the D/E/K/A pore signature. On the other hand, the differences in their amino acid sequences are considerable, implying differing functions of the isoforms and situation-dependent differential utilizations (tissue- or life stage-specific expression, etc.). A clearer sign of functional specificity is seen in the $Na_V2(Ca_V4)$ proteins; the one (depicted as Na_V2a in Fig. 4) contains a D/D/Q/A, not the D/E/E/A, pore signature at the ion-selectivity filter. Although we do not know the ion permeability of amphioxus Na_V2a, it is conceivable the D/D/Q/A signature invests the excitable membranes of this animal with a regulatory option. Examination of these organisms enables us to monitor an "evolutionary experiment" carried out through gene duplication before the emergence of vertebrates (Ohno 1970).

Similar traces are also found in the tunicate lineage, which possess four types of $Na_V1/Na_V2(Ca_V4)$ proteins. Ascidians, constituting a representative tunicate class, abundantly distribute along the shores around the world. Their adult form is sessile, while the larvae are in the form of tiny tadpoles that swim in the sea. Ascidians have been utilized as a research model, because of their kinship to vertebrates, but also because of their abundance and the availability of mature gametes among other

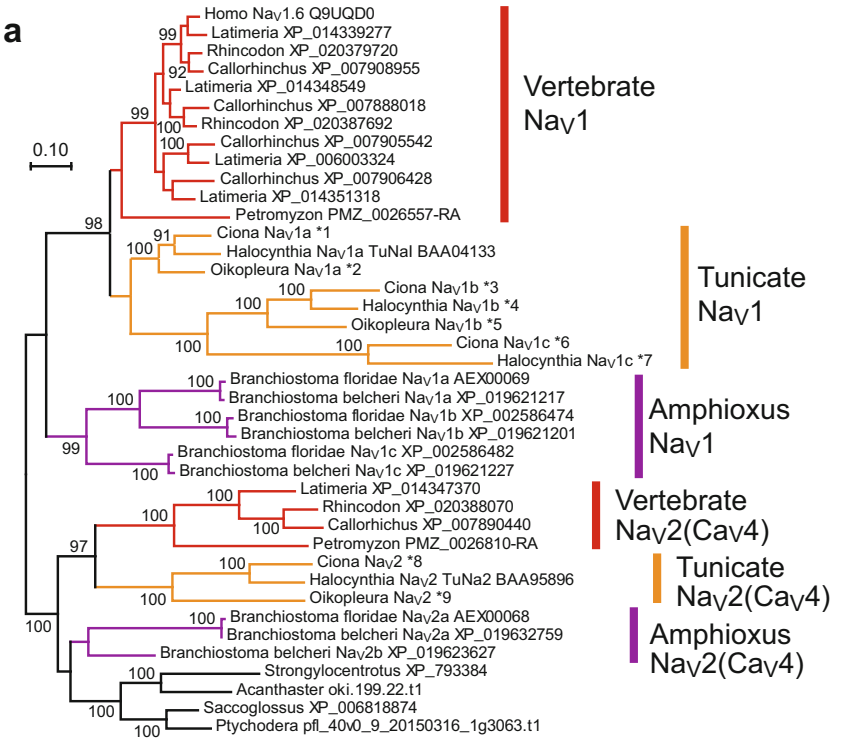

b

				Domain I II	Ankyrin-binding	III	Inactivation latch	IV
Amphioxus	Brabe	XP_019632759	Nav2a	TLDYF	CGDWV	LSLVSDKSEHSV	TFQGW	GYLDIFLTSNQ TSAGW
Amphioxus	Brabe	XP_019623627	Nav2b	TLDYW	CGEWI	SPRSASHAGSRA	TFEGW	ASIDLFLTETQ TSAGW
Ascidian	Cioin	*8	Nav2	TLDYW	CGEWI	LPRIVEEPSGEQ	TFEGW	SAVEALLTDNQ TSAGW
Ascidian	Halro	BAA95896	Nav2	TLDYW	CGEWI	KPESVEIREETP	TFEGW	SAVEAFLTESQ TSAGW
Larvacean	Oikdi	*9	Nav2	TLDFW	CGEWV	VDMLIGNCKSRL	TFEGW	SACDTIMTPEQ TSAGW
Lamprey	Petma	PMZ_0026810-RA		TIDYW	CGEWI	NPQIQESKSWSE	TLEGW	GALMALLTEDQ TAGGW
Chimaera	Calmi	XP_007890440		TLDYW	CGEWI	APLADCSTGPPK	TFEGW	GALVTLLTEDQ TAAAW
Shark	Rhity	XP_020388070		XXXXX	XXXXX	XXXXXXXXXXXX	TFEGW	GALVTVLTEDQ TAAAW
Coelacanth	Latch	XP_014347370		XXXXX	CGEWL	VPETLEEAQVDP	TFEGW	GALVILLTEDQ TAAGW
Amphioxus	Brabe	XP_019621217	NaV1a	VQDYW	CGEWV	VPIAGFDSELDI	TFKGW	SSIDLFMTEDQ TSAGW
Amphioxus	Brabe	XP_019621201	NaV1b	NQDFW	CGEWI	VEESKDENKDGN	TFKGW	SSADLFMTEDQ TSAGW
Amphioxus	Brabe	XP_019621227	NaV1c	TQDYW	CGEWI	TPVCNHRISEKG	TFKGW	DSEDLFMTEDQ TSAGW
Ascidian	Cioin	*1	NaV1a	AQDYW	CGEWI	VPIAALESDLEN	TFKGW	GGQDIFMTEEQ TSAGW
Ascidian	Halro	BAA04133	NaV1a	AQDYW	CGEWI	VPRADGESDFEV	TYKGW	GGQDIFMTEEQ TSAGW
Larvacean	Oikdi	*2	NaV1a	VQDYW	CGEWI	VPIKSSPVKERL	TFKGW	GGQDIFMTEEQ TSAGW
Ascidian	Cioin	*3	NaV1b	ALDSW	CGEWV	SPTSSSHRRRKA	TFTGW	GEDGVFLTDEQ TSEGW
Ascidian	Halro	*4	NaV1b	AQDAW	CGEWI	NSLRQGSDEKDS	TFKGW	GEDGVFLTDEQ TSEGW
Larvacean	Oikdi	*5	NaV1b	ALDAW	CGEWV	NEFSNGTSPTKS	TFMGW	FDDGVFLTDEQ TSEGW
Ascidian	Cioin	*6	NaV1c	LQDNW	CGEWI	TPSKRTESMDTV	TFKGW	AGTELFLTDTQ TSAGW
Ascidian	Halro	*7	NaV1c	LQDNW	CGEWI	QPDRLQIPLQPH	TFKGW	QTGALFLTESQ TSAGW
Lamprey	Petma	ABB84815		XXXXX	XXXXX	VPIAVGESDFET	TFKGW	GGQDIFMTEEQ XXXXX
Lamprey	Petma	ABB84816		XXXXX	XXXXX	VPIAKLEAELER	TFKGW	GGEDIFMTEEQ XXXXX
Lamprey	Petma	PMZ_0026557-RA		TQDYW	XXXXX	NRIIKYKCSLTK	TFKGW	GGEDIFLTEEQ TSAGW
Lamprey	Petma	PMZ_0026115-RA		TQDYW	CGEWI	VPIAVGESDFEN	TFKGW	XXXXXXXXXXX TSAGW
Chimaera	Calmi	XP_007905542		TQDFW	CGEWI	VPIAEPESDCEE	TFKGW	GGKDIFMTEEQ TSAGW
Chimaera	Calmi	XP_007908955		TQDFW	CGEWI	VPIAVGESDFEN	TFKGW	GGQDIFMTEEQ TSAGW
Chimaera	Calmi	XP_007906428		TQDFW	CGEWI	VPIAAVESYSEC	TFKGW	GGQDIFMTEEQ TSAGW
Chimaera	Calmi	XP_007888018		TQDCW	CGEWI	VPIAIGESDFEN	TFKGW	GGQDIFMTEEQ TSAGW
Shark	Rhity	XP_020387692		TQDYW	CGEWI	VPIALGESDFEN	TFKGW	GGQDIFMTEEQ TSAGW
Coelacanth	Latch	XP_014351318		TQDYW	CGEWI	VPIAIGESDSEY	TFKGW	SGEDIFMTEEQ TSAGW
Coelacanth	Latch	XP_014339277		TQDFW	CGEWI	VPIAVGESDFEN	TFKGW	GGQDIFMTEEQ TSAGW
Coelacanth	Latch	XP_014348549		TQDYW	CGEWI	VPIAVGESDFEN	TFKGW	GGQDIFMTEEQ TSAGW
Coelacanth	Latch	XP_006003324		TQDYW	CGEWI	VPIAAAESDLEI	TFKGW	GGKDIFMTEEQ TSAGW
Mammal	Homsa	Q9UQD0	NaV1.6	TQDYW	CGEWI	VPIAVGESDFEN	TFKGW	GGQDIFMTEEQ TSAGW

Fig. 4 Molecular phylogeny of chordate Na_V1 and $Na_V2(Ca_V4)$ channels. (**a**) A maximum-likelihood tree of Na_V-related channels from acorn worms (*Ptychodera flava*, *Saccoglossus kowalevskii*), the starfish (*Acanthaster planci*), the sea urchin (*Strongylocentrotus purpuratus*), amphioxi (*Branchiostoma belcheri* and *B. floridae*), ascidians (*Ciona intestinalis*, *Halocynthia*

features. Ascidians have contributed to ion channel studies through the "mosaicism" of their embryogenesis. Historical studies revealed that neuron-like Na^+ spikes could be evoked in the neural cell-lineage blastomere of embryos whose cleavage was arrested using an inhibitor of cytokinesis (Takahashi and Yoshii 1981; Takahashi and Okamura 1998). Developmental expression of this Na^+ current in the neural cell-lineage blastomere is dependent on a fibroblast growth factor-like inductive signal from a neighboring endomesodermal blastomere, which represents neural induction. This process of differentiation in membrane excitability is firmly correlated with the gene expression of a Na_V1 channel, originally called TuNaI (referred to as Na_V1a here) (Okado and Takahashi 1988; Okamura et al. 1994; Takahashi and Okamura 1998). This Na_V1a α subunit is actually expressed in all known neuronal types (Okamura et al. 1994; Okada et al. 1997). Later studies carried out before and after the genomic sequencing of several species of ascidians revealed that ascidians have four genes encoding Na^+ channel α subunits (Nagahora et al. 2000; Okamura et al. 2005; Brozovic et al. 2016). One encodes Na_V1a (TuNaI) containing the typical D/E/K/A pore signature, an inactivation latch with the I-F-M triplet between domains III and IV, and a sequence similar to the ankyrin-binding motif found in the loop between domains II and III of vertebrate Na_V1s (see below). Another encodes a $Na_V2(Ca_V4)$ subfamily protein containing the typical D/E/E/A pore signature (Na_V2, previously called TuNa2), but lacking clear consensus sequences for the inactivation latch and ankyrin-binding motif (Fig. 4) (Nagahora et al. 2000). This gene encoding $Na_V2(Ca_V4)$ is also expressed in some, but not all, neurons in ascidians (Nagahora et al. 2000). The nested patterns of Na_V1 and $Na_V2(Ca_V4)$ gene expression are reminiscent of the patterns of *para* and *DSC1* expression in *Drosophila* embryos (Hong and Ganetzky 1994).

Fig. 4 (continued) roretzi), the larvacean (*Oikopleura dioica*), the lamprey (*Petromyzon marinus*), the elephant fish chimaera (*Callorhinchus milii*), the whale shark (*Rhincodon typus*), the coelacanth (*Latimeria chalumnae*), and humans (*Homo sapiens*). The clades of Na_V1 and $Na_V2(Ca_V4)$ are clearly divided. Vertebrates possess $Na_V2(Ca_V4)$. The sequences from amphioxi, tunicates (ascidians and larvaceans), and vertebrates are labeled with *purple*, *yellow*, and *red* branches, respectively. NCBI accession numbers and other ID codes are mostly indicated in the tree. *1-*9 indicate the genemodel IDs in the genome browser of each organism: *1, KH.C9.462.v3.A.SL1–1; *2, GSOIDP00013476001; *3, KH.C1.1161.v1.A.ND1–1; *4, Harore.CG.MTP2014.S1.g14830; *5, GSOIDP00011229001; *6, KH.C10.502.v2.A.SL1–1; *7, Harore.CG.MTP2014.S25.g02359; *8, KH.C5.200.v1.A.ND1–1; *9, GSOIDP00005042001. The *O. dioica* sequences are obtained from OikoBase (http://oikoarrays.biology.uiowa.edu/Oiko/); the *C. intestinalis* sequences are from Ghost database (http://ghost.zool.kyoto-u.ac.jp/cgi-bin/gb2/gbrowse/kh/); the *H. roretzi* sequences are from Aniseed database (https://www.aniseed.cnrs.fr/); the *P. marinus* sequences are from the UCSC genome browser gateway (http://genome-asia.ucsc.edu/cgi-bin/hgGateway); and the *A. planci* and *P. flava* sequences are from the OIST genome browsers (http://marinegenomics.oist.jp/gallery/gallery/index). The bootstrap values over 90 are shown. The tree was constructed using the WAG model on MEGA7 from gap-free 526 amino acid positions aligned by MUSCLE program. (**b**) The pore signatures and the regions corresponding to ankyrin-binding motif and the inactivation latch in chordate Na_V-related channels. The species codes and color codes are as used in Figs. 2 and 3. Amino acids identical to the mammalian $Na_V1.6$ ankyrin-binding motif are indicated by *brown*. *1-*9: the genemodel IDs identical to those in (**a**)

The other two channels in ascidians, called here Na_V1b and Na_V1c (previously named Na_V3 and 4, respectively, in Okamura et al. 2005), are categorized in the Na_V1 family, and the tunicate Na_V1a, b, and c constitute a clade different from that including the vertebrate Na_V1s (Fig. 4a). While the ion-selectivity filter signature of the tunicate Na_V1c is the same as that in typical Na_V1-type channels (D/E/K/A), Na_V1b exhibits a D/E/(K or T or M)/E pore signature (Fig. 4b) (see also Widmark et al. 2011). We do not know the ion permeability of either channel. Temporal expression patterns estimated from the counts of expressed sequenced tags (ESTs) in the ascidian *Ciona intestinalis* (Satou et al. 2003) suggests the tunicate Na_V1a (TuNaI) is expressed in the larval and adult nervous systems which is consistent with in situ analyses of this gene expression pattern (Okamura et al. 1994, 2005; Okada et al. 1997). Na_V2 is estimated to be expressed in the nervous systems of larvae and juveniles, and possibly on the juvenile endostyle, which is an organ putatively homologous to the vertebrates' thyroid gland. The EST counts suggest expression of Na_V1b occurs during the larval stage. Our preliminary examination of the spatial expression pattern in *C. intestinalis* showed that the Na_V1b gene is expressed in neurons in the CNS and PNS and in some of the muscle cells in the larva. The EST counts predict a small amount of Na_V1c is expressed during the larval stage, though our preliminary in situ hybridization analysis did not detect any clear signal during the larval stage. Also, intriguing is the detection of EST counts for Na_V1b and Na_V1c in mature hermaphroditic adults producing gametes, not in young immature adults. In the eggs of ascidians, steep membrane depolarization is evoked in response to fertilization, which is known to be mediated by an unknown voltage-gated Na^+ channel that is somewhat permeable to Ca^{2+} along with Na^+ (Okamoto et al. 1977; Fukushima 1981; Okamura and Shidara 1987). Thus Na_V1b and/or Na_V1c may be involved in this process.

Single-channel recordings from cleavage-arrested neuronal blastomeres of the ascidian *Halocynthia roretzi* support this view. The electrophysiology has uncovered three types of voltage-gated sodium currents that turn over with time after fertilization to matured stage (Okamura and Shidara 1990a, b). The "Type A" Na^+ current shows only one decay phase during voltage-dependent inactivation, suggesting that a single type of Na_V is responsible for this current. Type A currents are seen in every blastomere within early embryos, and its expression level appears highest at the gastrula stage. This type of Na^+ current is identical to that in the fertilization potential of *Halocynthia* eggs represented by a Na^+-dependent AP (Fukushima 1981). The Na_V current in *Halocynthia* eggs is insensitive to TTX but is highly sensitive to scorpion toxin and local anesthetics (Okamoto et al. 1977). These data suggest that the tunicate Na_V1b, which has an atypical pore signature and is thus resistant to TTX, is involved in the Type A current. On the other hand, voltage-dependent inactivation of the "Type C" current shows two different, fast and slow, phases of decay (Okamura and Shidara 1987), which is reminiscent of the Nav1.6 channel in mammalian neurons. The Type C is the most predominant in differentiated neuronal blastomeres and is suppressed by microinjection of antisense DNA targeting the *Halocynthia* Na_V1a gene *TuNaI* (Okamura et al. 1994). During the short period between the disappearance of Type A and appearance of Type C currents during the

developmental course of neural-type membrane excitability, an unusual voltage-gated Na^+ current, "Type B," is transiently expressed (Okamura and Shidara 1990a). This current shows persistent gating behavior with multiple short openings (burst activity). At present, the relationship between the classically characterized diversity of voltage-gated Na^+ currents and the ascidian Na_V isoforms remains unclear, though it appears that Na_V1a (TuNa1) carries Type C current. It would be interesting to know whether the tunicate Na_V1b or Na_V1c carries the Type A current and what underlies the Type B current.

The tree topology shown in Fig. 4 suggests that the ancestor of tunicate Na_V1 paralogues became the seed from which there was further molecular evolution of the Na_V1 channels in modern vertebrates. The Na_V1a of tunicates shares an ankyrin-binding motif sequence with the vertebrate Na_V1s (Fig. 1) (Hill et al. 2008), which consists of a dozen amino acids residing in the loop between domains II and III (Fig. 4b), while the Na_V1b and Na_V1c proteins almost lost it. Similarly, the I-F-M inactivation latch that is conserved in the tunicate Na_V1a has been lost in the paralogues, Na_V1b and Na_V1c (Fig. 4b). Another ankyrin-binding motif similar to that in vertebrate Na_V1s is also found in vertebrate KCNQ2/3 ($K_V7.2/7.3$) K^+ channels, and these motifs are crucial for ankyrin-G binding and for anchoring of Na_V1s and KCNQ2/3s at the axon initial segment (AIS) and nodes of Ranvier in myelinated neurons (Garrido et al. 2003; Lamaillet et al. 2003; Pan et al. 2006; Hill et al. 2008). The sequences of the motif in ascidians' Na_V1a varies somewhat, but ~70% of the amino acids are conserved (Fig. 4b). Even the Na_V1 channel in amphioxi, depicted as *Branchiostoma* Na_V1a in Fig. 4, has ~40% identity, though we find no other traces in invertebrate Na_V1s (Fig. 4b) (Hill et al. 2008). Myelination and resultant saltatory conduction are regarded as a feature of jawed vertebrates (gnathostomes) (Zalc et al. 2008; Zalc 2016). Despite the absence of nodes of Ranvier in amphioxi and tunicates, the ankyrin-binding motif emerged in these animals and may have initiated interaction with ankyrins within neurons. This may be a key property that the ancestral gene of the tunicate Na_V1 paralogues retained, and the reason it was selected as the seed for further evolution in the vertebrate lineage.

The situations seen in amphioxi and tunicates inform us that the isoforms occurring in these so-called "protochordate" organisms through gene duplication differentially evolved, leading to changes, even into the pore signature (as seen in Na_V1b of tunicates and Na_V2b of amphioxi). The gene duplications can confer specific regulatory options to each of duplicated isoforms as indicated so far (Ohno 1970). What occurred in these organisms is a prelude to what has occurred in the vertebrate lineage: another story of gene duplication and functional differentiation.

6 Evolution of Na_V1 Channels in Vertebrates

The monophyletic vertebrate lineage has given rise to agnathans (hagfish and lampreys), cartilaginous fish (sharks, skates, and rays), ray-finned fish (bichirs, sturgeons, gars, bowfin, and teleosts), lobe-finned fish (paraphyletic group of

coelacanths and lungfish), and tetrapods (amphibians, reptiles, birds, and mammals) (e.g., Amemiya et al. 2013). During this process of radiation, these organisms inhabited and adapted to various environments in salt and freshwater and in wet and dry terrestrial areas. An ability for predation has been especially well developed in this animal lineage, and several ideas have been proposed in that regard (e.g., Gans and Northcutt 1983). Myelination and saltatory conduction along neuronal axons, as well as the developmental capacities derived from neural crest and placode cells that especially enhanced sensory systems, referred to as "new head," have enabled vertebrates to become larger and predatory (e.g., Gans and Northcutt 1983; Zalc 2016). The presence of active predators in turn stimulated greater ability to efficiently recognize the predators so as to escape (Parker 2003). Increased complexity of sensory inputs, higher ordered neural processing, and high-speed regulation of locomotion would have strongly supported the radiation of vertebrates under water and on land. Na_V1 function was definitely essential to those evolutionary steps.

The lamprey *Petromyzon marinus* shows multiple types of predicted transcripts encoding Na_V1 channel α subunits. Two Na_V1 isoforms have previously been identified (Hill et al. 2008; Zakon 2012), but four types, at least, may be there (Fig. 4b). Cartilaginous fish, including the elephant fish (chimaera) *Callorhinchus milii*, and the whale shark *Rhincodon typus* also appear to harbor four to five (or more) predicted transcripts for Na_V1 isoforms (Fig. 4; some sequences were too short and thus omitted here). Our molecular phylogenetic analysis suggests the Na_V1 isoforms in cartilaginous fish well reflect an original state (one gene in each of NaV1.4, NaV1.5/1.8/1.9, NaV1.6, and NaV1.1/1.2/1.3/1.7 groups), before the extensive duplication that occurred in amniotes and in teleosts (Figs. 4 and 5) (see below) (Widmark et al. 2011). It remains difficult, however, to know precise full-length sequence data for these transcripts, and there is not yet sufficient data available to draw firm conclusions.

Three lamprey Na_V1 α subunits for which longer sequence information was found in the database have the D/E/K/A pore signature. On the other hand, at least two of them contain the I-F-M inactivation ball in the loop between domains III and IV, while the third has an I-F-L triplet. The ankyrin-binding motif is conserved to varying degrees (50–100%) in their domain II-III loops (Fig. 4b). The variation in sequence motifs may represent differences of the molecular functions among them, which implies efficient "evolution by gene duplication" working in this gene family from the beginning of the vertebrate lineage (Ohno 1970).

The ankyrin-binding motif may reportedly work to locate and accumulate Na_V1s at the AIS in the neurons of lampreys (Hill et al. 2008). True myelin sheaths have not been found along the axons of lampreys, though molecular traces of myelination have been detected (Smith et al. 2013). On the other hand, the proximal portion of neuronal axons in lampreys is thinner than elsewhere along the axon. This narrow initial segment decreases local capacitance and conductance and supports the occurrence of steep APs. Localization of Na_V1 at high density in the AIS makes sense for efficient induction of APs (Hill et al. 2008; Kole and Stuart 2012), and full establishment of Na_V1 localization at the AIS via its ankyrin-binding motif may have facilitated the increase in body size of the vertebrate